NASA TECHNICAL NOTE

NASA TN D-6043

C. 1

LOAN COPY: RETUR
AFWL (WLOL)
KIRTLAND AFB, N

TECH LIBRARY KAFB, NM
0132799

NASA TN D-6043

VELOCITY, INTERMITTENCY, AND TURBULENCE INTENSITY MEASUREMENTS IN THE BOUNDARY LAYER OF AN ACCELERATED FLOW

by Donald R. Boldman, Harvey E. Neumann, and Robert C. Ehlers

Lewis Research Center
Cleveland, Ohio 44135

NATIONAL AERONAUTICS AND SPACE ADMINISTRATION • WASHINGTON, D. C. • OCTOBER 1970

TECH LIBRARY KAFB, NM
0132799

1. Report No. NASA TN D-6043	2. Government Accession No.	3. Recipient's Catalog No.
4. Title and Subtitle VELOCITY, INTERMITTENCY, AND TURBULENCE INTENSITY MEASUREMENTS IN THE BOUNDARY LAYER OF AN ACCELERATED FLOW		5. Report Date October 1970 6. Performing Organization Code
7. Author(s) Donald R. Boldman, Harvey E. Neumann, and Robert C. Ehlers		8. Performing Organization Report No. E-5689
9. Performing Organization Name and Address Lewis Research Center National Aeronautics and Space Administration Cleveland, Ohio 44135		10. Work Unit No. 129-01 11. Contract or Grant No.
12. Sponsoring Agency Name and Address National Aeronautics and Space Administration Washington, D. C. 20546		13. Type of Report and Period Covered Technical Note 14. Sponsoring Agency Code
15. Supplementary Notes		

16. Abstract

Boundary layer surveys of time-mean velocity, intermittency, and turbulence intensity were obtained in a 30° half-angle of convergence nozzle operating with air. The measurements were obtained by means of a constant temperature hot-wire anemometer. The tests, which were performed at adiabatic wall conditions, revealed some of the effects of strong acceleration on an initially turbulent boundary layer.

17. Key Words (Suggested by Author(s)) Turbulent boundary layer Turbulence Accelerated flow Intermittency	18. Distribution Statement Unclassified - unlimited		
19. Security Classif. (of this report) Unclassified	20. Security Classif. (of this page) Unclassified	21. No. of Pages 35	22. Price* $3.00

*For sale by the Clearinghouse for Federal Scientific and Technical Information
Springfield, Virginia 22151

VELOCITY, INTERMITTENCY, AND TURBULENCE INTENSITY MEASUREMENTS IN THE BOUNDARY LAYER OF AN ACCELERATED FLOW

by Donald R. Boldman, Harvey E. Neumann, and Robert C. Ehlers

Lewis Research Center

SUMMARY

Hot-wire surveys of the time-mean velocity, intermittency, and turbulence intensity were obtained in the boundary layer of an accelerated flow. The acceleration was provided by a 30° half-angle of convergence nozzle which operated with air. The tests were performed at room temperature and adiabatic wall conditions. Boundary layer surveys were obtained at stagnation pressures of 300 and 45 psia (207 and 31 N/cm^2, respectively). These pressures provided values of acceleration parameter below and above a critical value for "laminarization."

The results of this study indicated that a boundary layer in a highly accelerated flow differs from that in unaccelerated flow because the acceleration results in a mass discharge from the much thicker boundary layer occurring upstream. This mass discharge is referred to as a "detrainment" process. The effects of "detrainment" were evident in the measured time-mean velocity profiles, the intermittency, and the turbulence intensity distributions. Upon accounting for the effects of "detrainment," on these measurements, the turbulence intensity across the boundary layer in the nozzle was quantitatively similar to that for a nonaccelerated flow.

INTRODUCTION

The boundary layer in a highly accelerated nozzle flow exhibits certain characteristics which uniquely identify it with an acceleration process. Under certain conditions an initially turbulent boundary layer can revert to one which appears to be laminar or partially laminar (e.g., refs. 1 to 5), often referred to as "laminarization." The "laminarization" process has been associated with an acceleration parameter K, where

$$K = \frac{\nu_\infty}{U_\infty^2} \frac{dU_\infty}{dx} \qquad \text{(ref. 1)}$$

In reference 1, a critical value of the acceleration parameter ($K_{crit} \approx 3\times10^{-6}$) was derived. When $K > K_{crit}$, an initially turbulent boundary layer can revert to a "laminarized" boundary layer; however, if $K < K_{crit}$ throughout the acceleration process, the boundary layer is expected to remain turbulent.

An initially turbulent boundary layer can also remain turbulent during acceleration; however, if the acceleration forces are sufficiently high, the velocity profiles differ from classical profiles associated with nonaccelerated flows. The principal difference between the profiles for accelerated and unaccelerated flows occurs in an outer region between the inviscid free stream and the turbulent shear layer adjacent to the wall, as was shown in references 4 and 6. In reference 6, velocity profiles at several axial stations in a two-dimensional nozzle indicated that this outer region behaves like inviscid flow.

The "laminarization" phenomenon (refs. 1 to 5), as well as the outer region of the turbulent boundary layer (refs. 4 and 6), was observed on the basis of wall heat-transfer measurements and time-mean velocity surveys. However, these time-mean measurements did not adequately characterize the turbulence properties of the boundary layer. It was therefore desirable to supplement these results with measurements of the turbulence structure of the boundary layer. The only practical method of obtaining such information in the complex flow environment of the present study was through hot-wire anemometry techniques.

The current investigation represents an extension of the work reported in reference 4. In reference 4 measurements of the time-mean velocity boundary layer profile were obtained at Mach 0.08 in a 30° half-angle of convergence nozzle. The measurements were obtained at $K \approx 6\times10^{-6}$ and 9×10^{-7}, thus representing values above and below K_{crit}. A turbulent boundary layer existed at the nozzle entrance under conditions corresponding to both these values of K. The results of reference 4 revealed that the inner portion of the profile attained the velocity profile characteristics of a laminar boundary layer at a high value of acceleration parameter ($K \approx 6\times10^{-6}$). When the value of K at the nozzle survey station was reduced ($K \approx 9\times10^{-7}$), the time-mean velocity near the wall varied approximately as a 1/7-power of the distance from the wall, thus indicating a conventional type of turbulent boundary layer. However, where the velocity was within a few percent of the free-stream value, the slope of the distribution was nearly an order of magnitude less than that of the wall region.

In the present study, certain turbulence properties, as well as the mean velocity profiles associated with the turbulent and "laminarized" boundary layers in a nozzle, were examined. Specifically, the distributions of the average velocity in the mean flow

direction U, the turbulence intensity u', and the intermittency factor γ were measured at the Mach 0.08 station in the 30° half-angle of convergence nozzle of reference 4. The working fluid was air which entered the nozzle at room temperature. The measurements were obtained with a constant temperature hot wire. Measurements of $\overline{uv}$ and $\sqrt{\overline{v^2}}$ could not be obtained because of the extremely thin boundary layer in the nozzle.

EXPERIMENTAL APPARATUS

The tests were performed in a 30° half-angle of convergence by 15° half-angle of divergence nozzle (fig. 1). A 6.5-inch (16.5-cm) diameter, 17.0-inch (43.2-cm) long

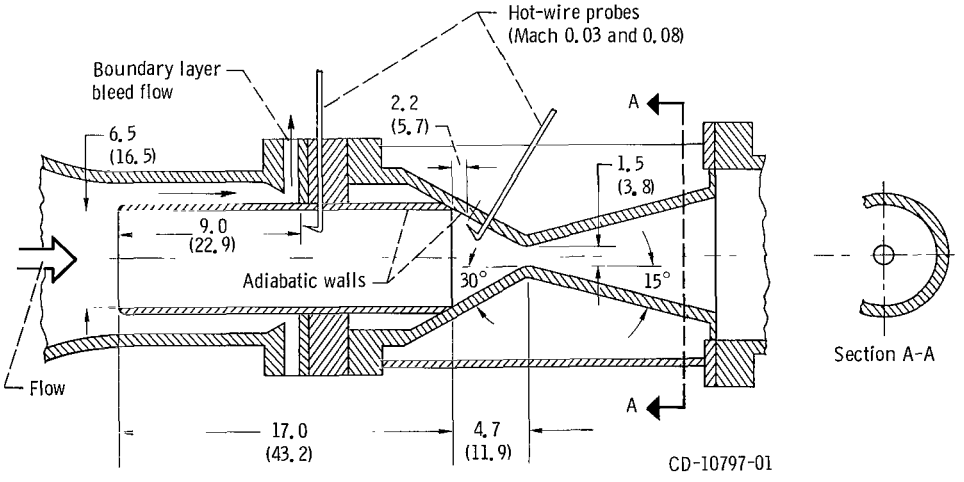

Figure 1. - Nozzle configuration. (Dimensions are in inches (cm).)

pipe inlet was coupled to the nozzle which was operated at adiabatic wall conditions. The inlet flow Mach number was nominally 0.03. A boundary layer bleed system was employed in order to initiate the turbulent boundary layer near the leading edge of the inlet. Room-temperature air was supplied at stagnation pressures of 45 and 300 psia (31 and 207 N/cm^2, respectively). These pressures produced differences in the acceleration sufficient to provide a turbulent boundary layer at 300 psia (207 N/cm^2) and a "laminarized" boundary layer at 45 psia (31 N/cm^2).

A constant temperature hot-wire anemometer was utilized in the measurement of mean velocity U, intermittency factor γ, and turbulence intensity u', in the boundary layer region of the flow field. The hot-wire probes were positioned so that the hot wire traveled in a direction normal to the nozzle wall. The boundary layer surveys in the

nozzle were performed at a station having a Mach number of 0.08.

The sensing element (hot wire) was made of 0.0002-inch (0.0005-cm) diameter by 0.10-inch (0.25-cm) long tungsten wire. The ends of the wire were copper plated and soldered to needle-point conductors as shown in figure 2. Alinement of the wire relative to the nozzle was established by means of a cathetometer.

The intermittency factor was measured with an electronic circuit of the type proposed by Bradbury in reference 7. This circuit, which featured a direct readout of intermittency factor, was relatively simple to use. In using the intermittency circuit, it was necessary to match the output of a Schmitt trigger with either the filtered or rectified turbulence signal, as shown typically in figure 3. The filtered and rectified

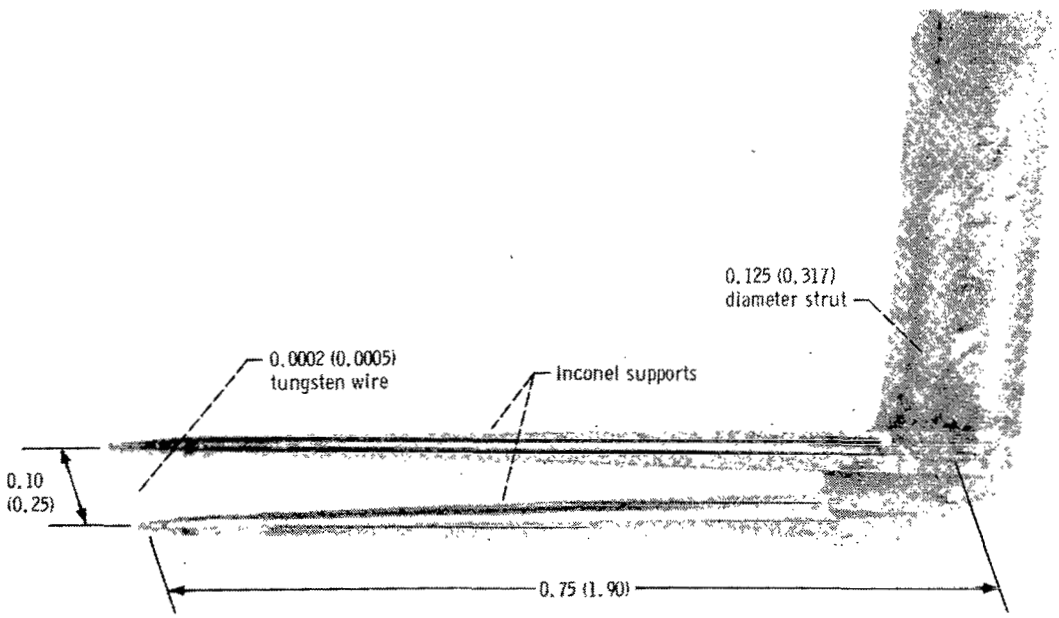

C-69-859

Figure 2. - Hot-wire probe. (Dimensions are in inches (cm).)

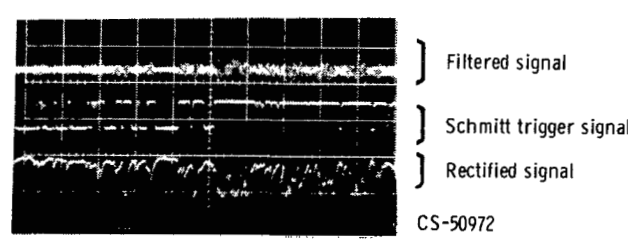

Time, 5 msec/division

Figure 3. - Typical signals from intermittency circuit. (Photographed from true dual-beam oscilloscope; trigger and rectified signals in chopped mode.)

signals denote the presence of "bursts" of high-frequency turbulence which can readily be distinguished from the signal for the inviscid free-stream flow over a large portion of the profile. The Schmitt trigger is a regenerative bistable device whose output depends on the amplitude of the incoming signal. The incoming signal is adjusted so that the duration of the constant amplitude pulses from the Schmitt trigger matches the duration of the turbulent bursts. This triggering or matching of signals obviously involves an element of subjectiveness; however, with the exception of the inner portion of the intermittent zone (where γ approaches 1.0) the matching of signals did not present a problem. The matching of signals was facilitated through the use of a true dual-beam oscilloscope.

The intermittency meter was first tested in a free-jet flow. The purpose of these tests was to (1) acquire a familiarity with the operation of the instrument and (2) to calibrate the meter. The calibration was based on a corroboration of the results with the well-established intermittency distributions for free jets. Such results have been presented, for example, in reference 8 where it was shown that the intermittency across the jet is accurately described by a Gaussian integral curve. In general, the present data for the free jet were within ±3 percent of the error function distribution of intermittency factor.

The intermittency circuit was then employed in measurements of γ across the boundary layer in the accelerated flow of the nozzle. Assessment of the accuracy of the measurements in the nozzle is difficult since, to the author's knowledge, similar measurements in highly accelerated flows are unavailable for comparison. If the free-jet results are used as an indication of measurement accuracy, an error band of ±3 percent should be assigned to the results. The establishment of two limiting conditions for intermittency factor lends additional credence in the data, particularly at the high-Reynolds-number operating condition. These limiting conditions are as follows: (1) near the wall the value of γ should approach unity, and (2) far from the wall (free stream) the value of γ should approach zero. It will be shown that these limiting criteria were satisfied at the high-Reynolds-number operating conditions where "laminarization" was not evident. However, at the low Reynolds number operating conditions where the boundary layer became laminarized it was difficult to establish the upper limit of γ with the intermittency circuit. The near-wall intermittency measurements associated with the "laminarized" boundary layer will therefore be analyzed only on a qualitative basis.

The probe was traversed point-by-point starting in the free stream and proceeding to the wall. The hot wires were usually destroyed upon contacting the wall; however, contact was necessary in order to determine the position coordinate for the measurements (distance from the wall y) with acceptable accuracy. The measured values of y in the wall region are estimated to be within 0.0005 inch (0.0013 cm) of the true position. This estimate is based on the linearity characteristics of the motor-driven actuator.

RESULTS AND DISCUSSION

The boundary layer profiles of the present investigation were measured at room temperature with adiabatic wall conditions. The results of these surveys, however, were similar to the boundary layer profiles of reference 4 which were measured with heated air and a cooled nozzle wall. The heat-transfer results of reference 4 revealed that pronounced changes in heat transfer can accompany the "laminarization" phenomenon. Before examining the boundary layer profiles measured with a hot wire, it is of interest to briefly review the heat transfer results of reference 4 for the Mach 0.08 survey station. The heat transfer is presented in terms of the Stanton-Prandtl number grouping $St_r Pr^{0.7}$ as a function of Reynolds number $Re_{d,r}$ in figure 4. "Laminari-

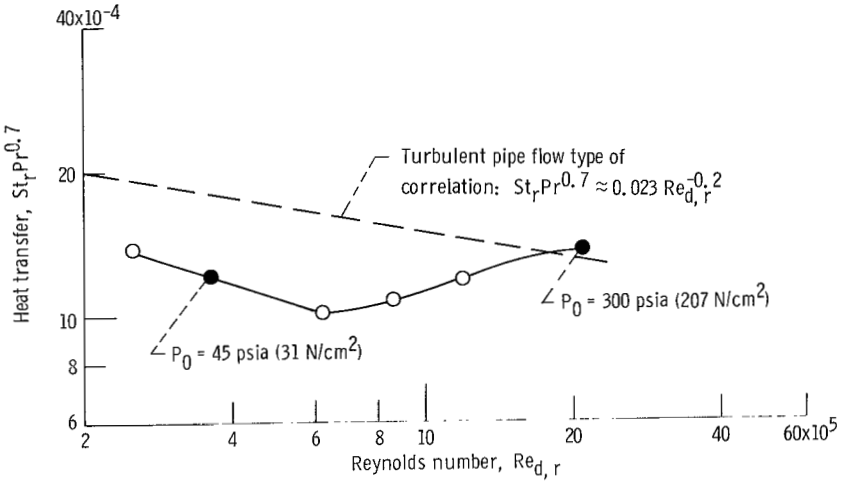

Figure 4. - Local heat transfer at survey station in nozzle. (Data from ref. 4.) Mach 0.08; stagnation temperature, 960° R (543 K).

zation" can be observed at the lower Reynolds number conditions ($Re_{d,r} < 2.0\times10^6$) as a reduction in $St_r Pr^{0.7}$ from a reference level based on pipe flow. The hot-wire measurements of the present study were obtained at stagnation pressures of 45 and 300 psia (31 and 207 N/cm^2, respectively) which correspond to Reynolds numbers of about 3.6×10^5 and 2.1×10^6, respectively. These conditions are denoted by the solid symbols in figure 4.

Mean Velocity Profiles

Pipe inlet. - The profiles of mean velocity in the pipe inlet are shown in figures 5

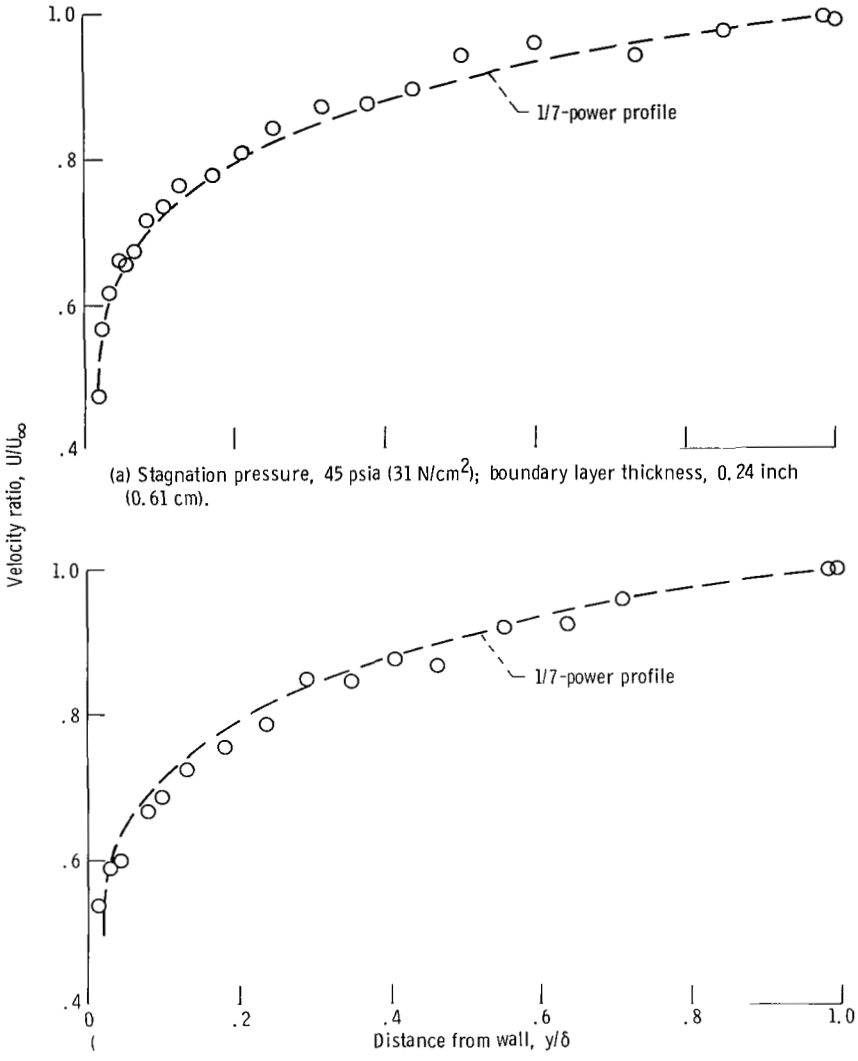

(a) Stagnation pressure, 45 psia (31 N/cm^2); boundary layer thickness, 0.24 inch (0.61 cm).

(b) Stagnation pressure, 300 psia (207 N/cm^2); boundary layer thickness, 0.18 inch (0.46 cm).

Figure 5. - Hot-wire measurements of mean velocity profiles in pipe inlet. Mach 0.03; stagnation temperature, 550° R (305 K); time-mean value of free-stream velocity, 36 feet per second (11 m/sec).

and 6. Results are given for stagnation pressures of 45 and 300 psia (31 and 207 N/cm^2, respectively). The hot-wire measurements of the velocity profiles are in good agreement with the 1/7-power law, and the law-of-the-wall representations at both pressure levels. The results are also consistent with those of reference 4 which were based on pitot probe measurements. Since the flow is not accelerated between the inlet probe station and the nozzle entrance, the classical turbulent structure of the boundary layer is expected to be maintained at least into the entrance region of the nozzle (plane of

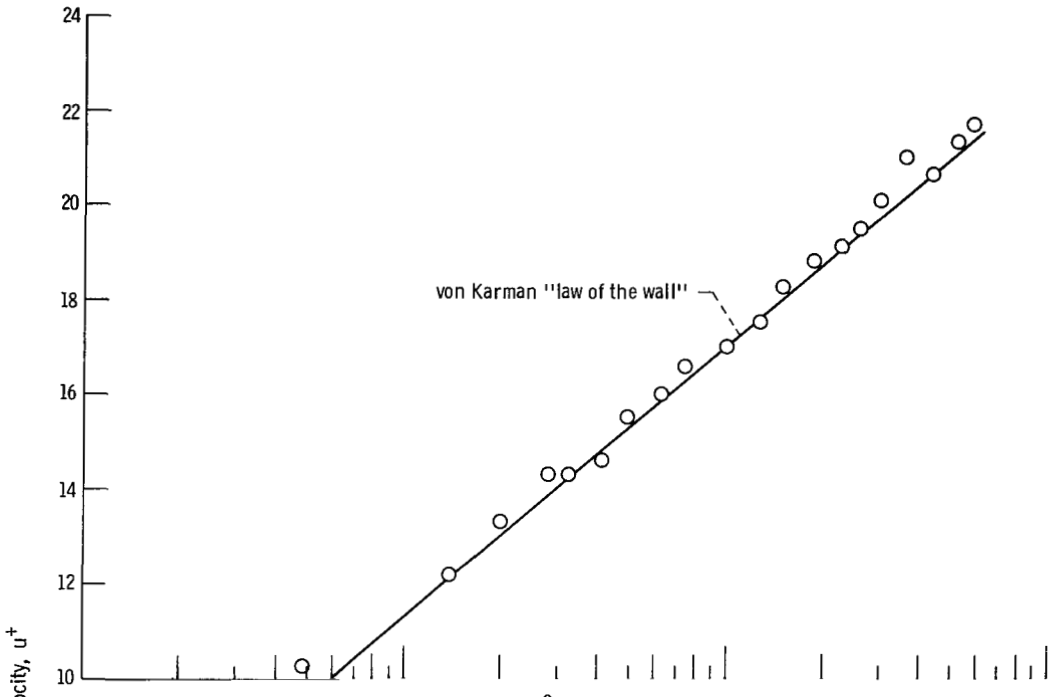

(a) Stagnation pressure, 45 psia (31 N/cm^2); skin friction coefficient, $C_f/2 = 0.00212$.

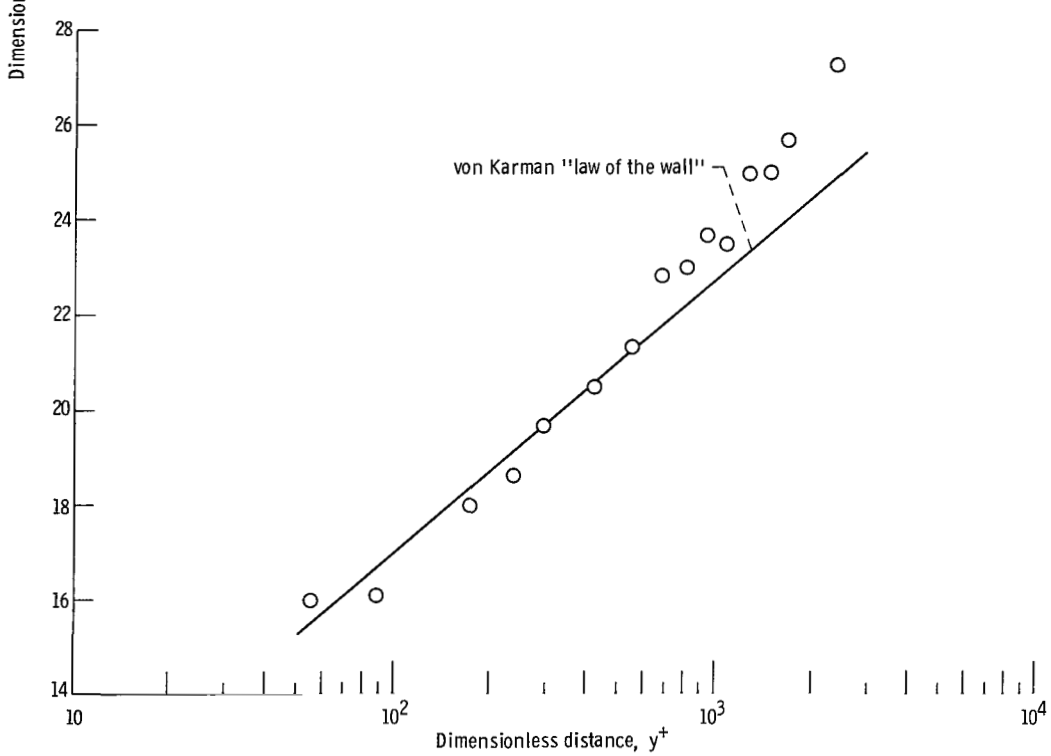

(b) Stagnation pressure, 300 psia (207 N/cm^2); skin friction coefficient, $C_f/2 = 0.00144$.

Figure 6. - Hot-wire measurements of mean velocity profiles in pipe inlet in terms of dimensionless distance and velocity. Mach 0.03; stagnation temperature, 550° R (305 K); time-mean value of free-stream velocity, 36 feet per second (11 m/sec).

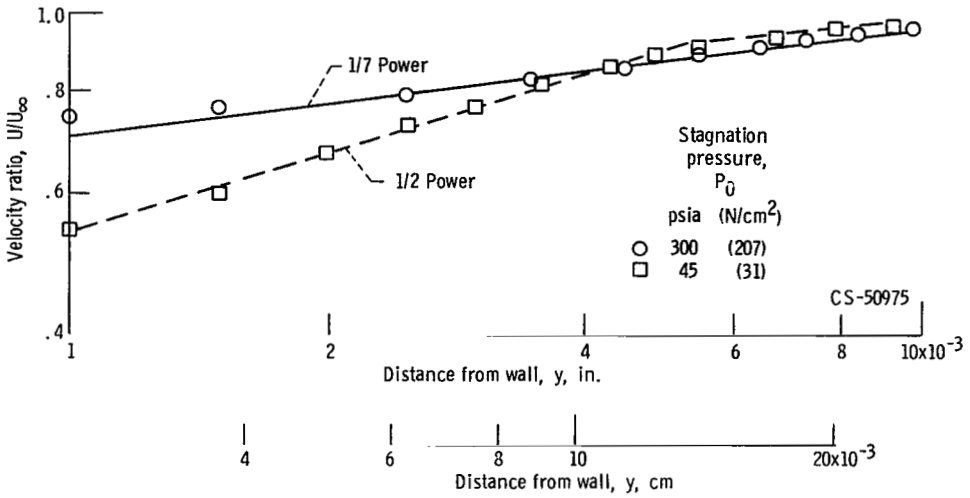

Figure 7. - Hot-wire measurements of inner portion of mean velocity profiles in nozzle showing effect of stagnation pressure (Reynolds number). Mach 0.08; stagnation temperature, 550° R (305 K); time-mean value of free-stream velocity, 92 feet per second (28 m/sec).

intersection between the pipe inlet and the conical nozzle).

Nozzle. - The corresponding mean velocity profiles in the nozzle are presented in figures 7 and 8. These profiles are consistent with the pitot probe measurements of velocity presented in reference 4 from the standpoint of (1) a change in the slope of the inner portion of the profile which accompanied the change in Reynolds number of acceleration parameter K (fig. 7) and (2) a long wake-type region comprising velocities greater than about 97 percent of the free-stream value (fig. 8). In the high stagnation pressure tests, the value of the acceleration parameter K at the nozzle survey station was 9×10^{-7}, which is appreciably below the previously mentioned critical value for "laminarization" of about 3×10^{-6}. The value of K corresponding to the low stagnation pressure tests was about 6×10^{-6}, which obviously exceeds the critical value. Therefore it appears from the hot-wire measurements of the profiles that "laminarization" can be observed independent of the amount of wall cooling.

The dominant effect on the velocity profile resulting from a change in the stagnation pressure (Reynolds number or acceleration parameter) occurs in the region of from 0.001 to about 0.010 inch (0.0025 to 0.025 cm), as shown in figure 7. At the high stagnation pressure condition, a large portion of the profile in this region is described by a 1/7-power law. The change in slope from a value of 1/7 to a value of 1/2 is ascribed to an acceleration-induced "laminarization" phenomenon which became apparent upon reducing the stagnation pressure. The 1/2-power variation in velocity appears to terminate at y = 0.005 inch (0.013 cm), after which the velocity profile is somewhat similar to that of the turbulent boundary layer. Therefore the profile cannot be considered to be

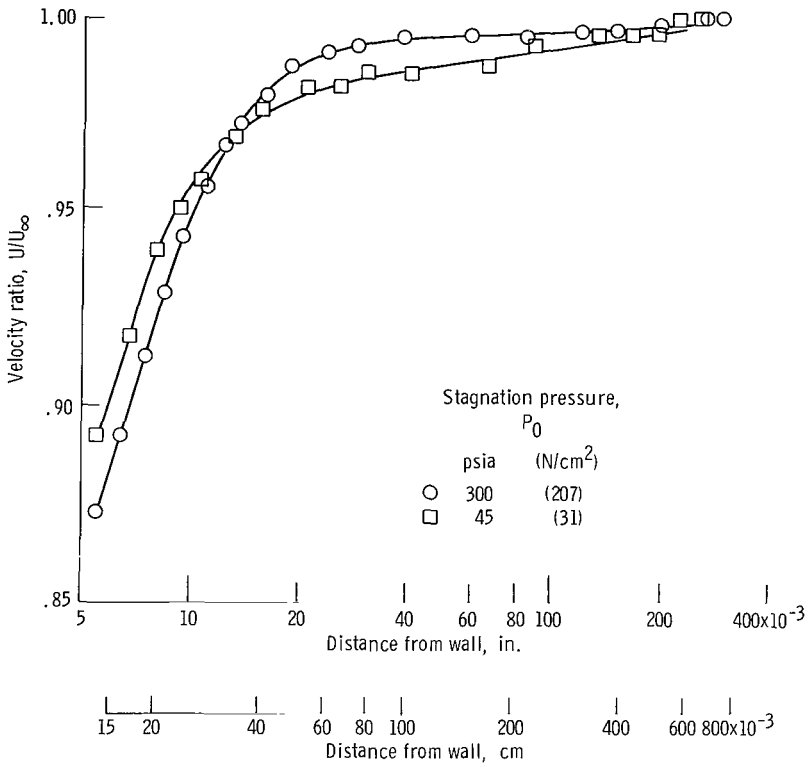

Figure 8. - Hot-wire measurements of outer portion of mean velocity profiles in nozzle showing effect of stagnation pressure (Reynolds number). Mach 0.08; stagnation temperature, 550° R (305 K); time-mean value of free-stream velocity, 92 feet per second (28 m/sec).

characteristic of a laminar boundary layer, but rather it appears to exhibit the time-mean characteristics of both a laminar and a turbulent boundary layer.

The velocity variation in the outer portion ($y \geq 0.020$ in. (0.051 cm)) of the two profiles in figure 8 is much more gradual than the 1/7-power and 1/2-power variations of the inner portions. Similar observations have also been reported in references 4 to 6. The resulting gradual increase in velocity with increasing distance from the wall is believed to be the result of a negative mass entrainment characteristic, that is, the movement of fluid out of the boundary layer into the free stream.

In the development of a boundary layer not subjected to acceleration, mass is continuously entrained into the boundary layer as it grows. All significant viscous effects occur in this layer. However, when strong acceleration forces are present, two distinct phenomena occur simultaneously. The boundary layer thins when the pressure forces dominate the viscous forces, and the size of the inviscid subsonic free-stream tubes contract because of the acceleration. As illustrated in figure 9, when the thinning effect of the boundary layer is greater than the stream tube contraction effect, mass can leave the boundary layer. A discussion of this phenomenon has also been presented in refer-

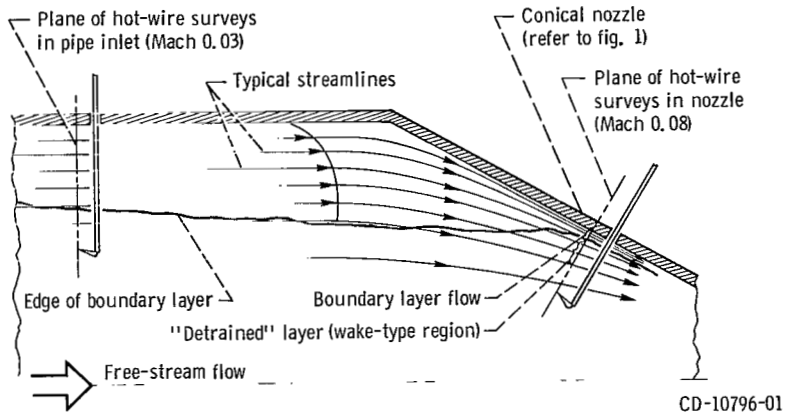

Figure 9. - Model of flow in entrance region of conical nozzle which is preceded by a pipe inlet.

ence 9 where the process was called "negative entrainment." In this study the authors have elected to refer to this phenomenon as a "detrainment" process.

"Detrainment" Criterion

The feasibility of "detrainment" of mass from a boundary layer can readily be illustrated for incompressible flow by starting with the following form of the integral momentum equation:

$$\frac{d}{dx} \ln \rho_\infty U_\infty \theta = \frac{C_f}{2\theta} - \left(\frac{\delta^*}{\theta} + 1 \right) \frac{d}{dx} \ln U_\infty$$

The mass flow in the boundary layer is

$$\dot{m} = \rho_\infty U_\infty (\delta - \delta^*)$$

"Detrainment" will occur when $d\dot{m}/dx$ becomes negative. In order to show that "detrainment" is, at least in principle, feasible, a power profile similarity will be assumed. The mass flow in the boundary layer can then be expressed as

$$\dot{m} = C \rho_\infty U_\infty \theta$$

where the constant C is given by $C = (\delta - \delta^*)/\theta$. It should not be inferred that $(\delta - \delta^*)/\theta$ is actually constant in a highly accelerated flow; however, this quantity should not vary

appreciably, especially upstream of the point of incipient "detrainment." Substitution of $\dot{m}$ into the momentum equation gives

$$\frac{d}{dx} \ln \dot{m} = \frac{C_f}{2\theta} - \left(\frac{\delta^*}{\theta} + 1 \right) \frac{d}{dx} \ln U_\infty$$

"Detrainment" will occur when $d\dot{m}/dx < 0$, or when

$$(\delta^* + \theta) \frac{d}{dx} \ln U_\infty > \frac{C_f}{2}$$

For small acceleration, the shear can dominate the pressure forces and no "detrainment" will occur. When the acceleration, as described by $(\delta^* + \theta)\, d(\ln U_\infty)/dx$, becomes greater than the friction coefficient, mass will begin to leave the boundary layer.

Model of the "Detrained" and Boundary Layers

When mass is "detrained," a layer is formed between the boundary layer and the inviscid free stream, as shown in figure 9. In reference 6 it was determined that this "detrained" layer (outer region) was a layer of negligible turbulent shear. A small radial total pressure gradient (or velocity gradient) is present in this layer of "detrained" fluid because of the upstream boundary layer history effect on the fluid. This effect becomes apparent upon considering the flow associated with the streamlines in the detrained layer (fig. 9). It should be noted that these streamlines emanated from a thick boundary layer at the nozzle entrance. The total pressure along a given streamline within the upstream shear flow region decreases as the flow progresses downstream. This reduction in total pressure occurs until the boundary layer "detrains" fluid. As was demonstrated in reference 6, the total pressure along a streamline within the "detrained" layer is essentially invariant. The flow in this layer is therefore rotational and approximately inviscid.

Although the "detrained" fluid can be treated as inviscid, residual turbulence is expected to be present. This residual turbulence can influence the measurements of intermittency factor and turbulence intensity in the boundary layer. However, before discussing these measurements, it is important to understand the model of the flow which crosses a hot wire fixed at some position near the wall. This model, presented in figure 10, consists of the free stream, the "detrained" layer, and a region which will be called the boundary layer. This division of the flow was chosen so that the usual laws

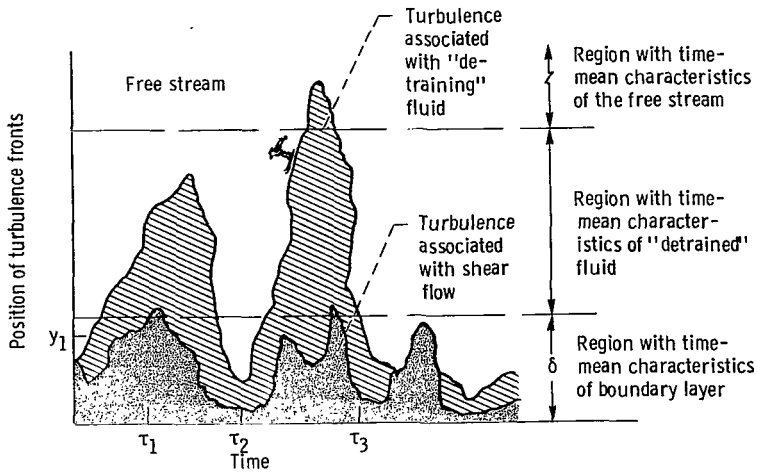

(a) Composite profile at fixed axial position in nozzle.

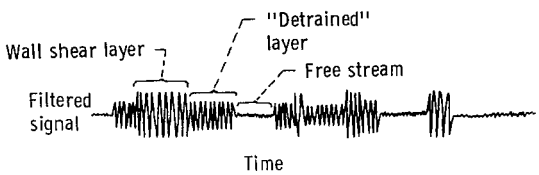

(b) Hot-wire signal at y_1 based on composite profile of figure 10(a).

Figure 10. - Model of flow in wall region of nozzle.

of the wall and wake for conventional boundary layer theory are maintained in the boundary layer region. Turbulence is present in the three regions composed of a wall shear flow, "detrained" flow, and free stream, as shown in figure 10(a). These three regions are assumed to be instantaneously separated by sharp lines of demarcation, each of which represents a turbulence front. The turbulence intensity of the free stream is much less than that of the "detrained" and wall shear fluids. A hot wire placed at $y = y_1$, (fig. 10(a)) is exposed to the different levels of turbulence associated with the three regions. For example, at time τ_1 the wire senses the turbulence in the wall shear layer. At time τ_2 the wire is in a region of low level free stream turbulence whereas at time τ_3 the wire is in a region of "detrained" fluid. The filtered signal from a hot wire placed at $y = y_1$ (fig. 10(a)) might be of the type shown in figure 10(b). The filtered signal associated with the "detrained" layer is depicted as being similar to the signal for the wall shear layer. Because of the bistable nature of the intermittency circuit, it can be used to distinguish between only two levels of turbulence, whereas the model of figure 10 indicates the possibility of three distinct levels of turbulence. In this case the intermittency circuit provides a distinction between the low-level free-stream turbulence and the higher levels of turbulence associated with the flow in the "detrained"

layer and wall shear regions. Therefore the measured values of intermittency factor are representative of the fraction of time that turbulence was present in the "detrained" fluid and/or the wall shear flow.

The turbulence intensity measured at the position $y = y_1$ (fig. 10(a)) represents an average of the turbulence intensity associated with each type of flow passing the wire. Therefore in order to determine the turbulence intensity associated with the wall shear flow, it is necessary to relate this turbulence intensity of the mixed flow, which the hot-wire measurements provide, to the intensities associated with each of the various types of flow and the associated intermittency factor (fraction of time present). The development of this relation is discussed in detail in the section Turbulence Intensity.

The time-mean characteristics of the three types of flow in the wall region can be separated and classified according to regions having a certain height, as shown in figure 10(a). The inner region represents the portion of the flow in which wall shear effects are predominant and is therefore called the boundary layer. This region is denoted by a thickness δ which is a rather arbitrary quantity.

The second region, which possesses the time-mean characteristics of the "detrained" fluid, extends from the edge of the boundary layer to the free stream (or third) region. The "detrained" region can be rather extensive (as in the present study), possibly orders of magnitude greater than the boundary layer thickness δ.

The flow at the edge of the "detrained" and boundary layers is a mixed flow. At the edge of the detrained layer, the mixed (intermittent) flow comprises "detrained" and free-stream fluid, whereas at the edge of the boundary layer δ the intermittent flow contains fluid from the wall shear, "detrained," and free-stream regions.

Intermittency Factor

The experimental studies of reference 8 and others have shown that the intermittency factor of a nonaccelerated boundary layer can be described by a Gaussian integral curve. The Gaussian integral distribution forms a straight line when plotted on a probability scale. The use of probability paper thus facilitates interpretation and comparison of intermittency data with the reported work for nonaccelerated flows.

The radial distribution of the experimental intermittency factor γ at the nozzle survey station is shown on probability paper in figure 11. These results are based on tests at two stagnation pressures; namely, 300 and 45 psia (207 and 31 N/cm^2, respectively). The flow in the "detrained" layer ($y > 0.03$ in. (0.08 cm)) is obviously intermittent; however, the distribution of γ is not described by a conventional Gaussian integral curve, as evidenced by the highly nonlinear variation on the probability scale. In the near-wall region ($y \lesssim 0.03$ in. (0.08 cm)), the intermittency factor shows a sud-

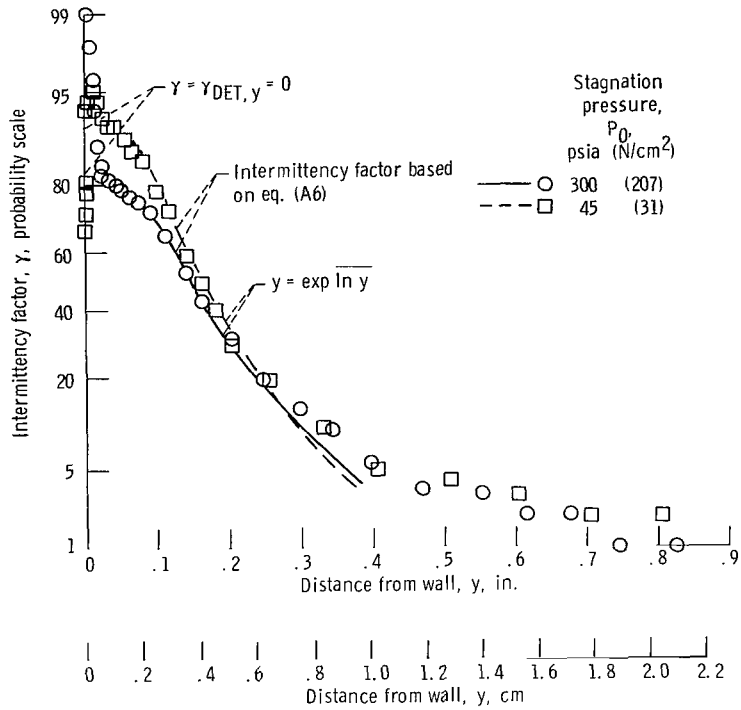

Figure 11. - Radial distribution of intermittency factor. Mach 0.08; stagnation temperature, 550° R (305 K).

den change in slope at both pressure levels. The location of this abrupt change in the slope of the intermittency distribution is significant from the standpoint of defining a boundary layer thickness δ.

Traditionally, δ was defined as the point where the time average velocity reaches some arbitrary percent, say 99 percent, of the free-stream velocity. However, this definition would lead to a very ambiguous and misleading quantity in the present study since δ would be some point near the outer edge of the "detrained" layer. A more meaningful value of δ can be obtained from the intermittency distribution of figure 11. It is believed that the points of discontinuous slope represent the boundary between the "detrained" layer and boundary layer and therefore will be used to define the thickness δ. The values of δ obtained in this manner are 0.024 inch (0.061 cm) for the high-pressure results and 0.030 inch (0.076 cm) for the low-pressure results. These boundary layer thicknesses coincide with the beginning of the gradual variation in velocity in the outer part of the profiles, as shown in figure 8. The abrupt change in the slope of the intermittency distribution at $y = \delta$ is emphasized in figure 12, where γ is presented as a function of the nondimensional distance y/δ.

The intermittency factor distributions in two equilibrium boundary layers measured by Klebanoff (ref. 10) and by Bradshaw (ref. 11) are also shown for comparison in fig-

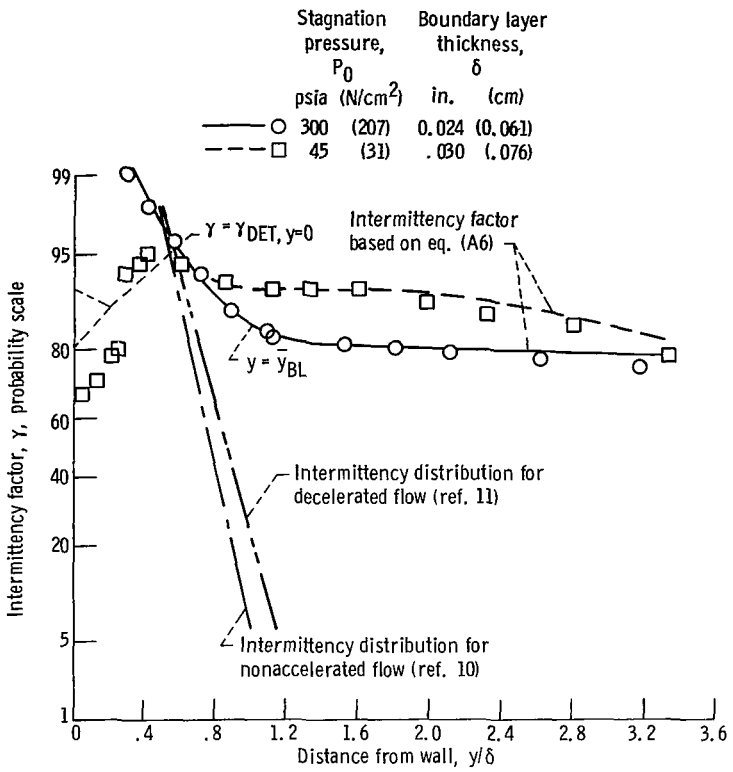

Figure 12. - Distribution of intermittency factor in nozzle boundary layer. Mach 0.08; stagnation temperature, 550° R (305 K).

ure 12. The data of Klebanoff are for a constant pressure boundary layer, whereas the data of Bradshaw are for an equilibrium boundary layer with an adverse pressure gradient. Both of these intermittency distributions can be closely approximated by complimentary error functions. For example, Klebanoff fitted his data to

$$\gamma = \frac{1}{2}\left[\operatorname{erfc} 5\left(\frac{y}{\delta} - 0.78\right)\right] \tag{1}$$

In this complimentary error function, the mean value of intermittency factor $\bar{\gamma}$ is attained at $y = 0.78\ \delta$. The standard deviation σ which is indicative of the eddy size, was determined to be equal to $0.14\ \delta$. The intermittency distribution for the adverse pressure gradient flow of reference 11 has a mean value of $\bar{\gamma}$ at $y = 0.87\ \delta$ and a standard deviation of $0.18\ \delta$. The larger standard deviation of the latter type of flow implies that the boundary layer with an adverse gradient has larger sized eddies.

The data for the high-pressure (300 psia (207 N/cm^2)) operating condition in figure 12 can also be approximated by a Gaussian integral curve within the boundary layer ($y/\delta \leq 1.0$). As shown in appendix A, the mean value of γ was at $y = 0.8\ \delta$ and the standard

deviation σ was equal to 0.12 δ. These values of the mean intermittency factor and standard deviation for the accelerated flow are similar to those of Klebanoff (ref. 10) for an unaccelerated flow.

The data at the 45 psia (31 N/cm^2) operating condition in figure 12, suggest that γ may vary as a Gaussian integral curve in the outer part of the boundary layer which extends from $0.4 \leq y/\delta \leq 1.0$. However, at $y/\delta < 0.4$, the distribution of γ changes and the intermittency factor decreases as the wall is approached. The authors consider this low-pressure intermittency data within the boundary layer to be only of qualitative value. As mentioned in the apparatus section, the intermittency meter could not be used with a high degree of confidence at the low pressure level because of problems in establishing an accurate value for the upper limit of intermittency factor. The qualitative trends, however, are expected to be correct.

The rapid reduction in γ with decreasing distance in the region of $y/\delta < 0.4$ ($y < 0.012$ in. (0.031 cm)) is due to "laminarization" of the boundary layer. However, the time-average velocity shown in figure 8 appeared to still have a turbulent-type profile at $y < 0.012$ inch (0.031 cm), suggesting that the acceleration has a stronger effect on the turbulent structure than on the time-mean characteristics of the flow.

The effects of intermittency have been shown to be important in considerations of predictions of turbulent transport. In reference 12, Baronti develops a phenomenological theory for incompressible boundary layers based on an eddy viscosity model. He demonstrates the necessity of including the intermittency in his eddy viscosity model. In order to account for the effects of intermittency in an eddy viscosity model, it is desirable to determine the functional form of the distribution. This has been done for nonaccelerated flows in the work of references 10 and 11 cited previously. An expression for the distribution of intermittency factor in the highly accelerated flow of the present study has been derived in appendix A. There the intermittency distributions for the boundary layer and the "detrained" layer are fitted to a single relation given by equation (A6), as

$$\gamma = \frac{\gamma_{DET,y=0}}{2} \operatorname{erfc}\left[\frac{\sqrt{\pi}\, e^{\overline{\ln y}}}{\gamma_{DET,y=0}}\left(-\left.\frac{\partial \gamma_{DET}}{\partial y}\right|_{y=e^{\overline{\ln y}}}\right)(\ln y - \overline{\ln y})\right] + \frac{1 - \gamma_{DET,y=0}}{2} \operatorname{erfc}\left(\sqrt{\pi}\, \frac{\bar{y}_{BL} - y}{1 - \gamma_{DET,y=0}} \left.\frac{\partial \gamma_{BL}}{\partial y}\right|_{y=\bar{y}_{BL}}\right)$$

The distribution of γ based on this expression is a combination of a log-normal and a Gaussian integral distribution, as shown in figures 11 and 12. Although this relation

closely fits the data presented herein, additional intermittency data should be obtained to verify the generality of the proposed function and to determine the acceleration effects on the coefficients.

Turbulence Intensity

The experimental distributions of turbulence intensity $u'(u' \equiv \sqrt{\overline{u^2}}/U_\infty)$ are presented in figure 13 for the high and low stagnation pressure operating conditions. A higher value of peak turbulence intensity occurred at the low-pressure operating condition in which "laminarization" was observed. In seeking an explanation for the high peak value of u' associated with "laminarized" flow, the results of reference 3 were examined. The data of reference 3 were obtained in an accelerated flow over a flat plate; however, the boundary layer in reference 3 did not appear to "detrain" fluid, as evidenced by the lack of an abnormal wake in the time-mean velocity profiles. The study of reference 3 revealed that the peak intensity measured when the value of K was near the

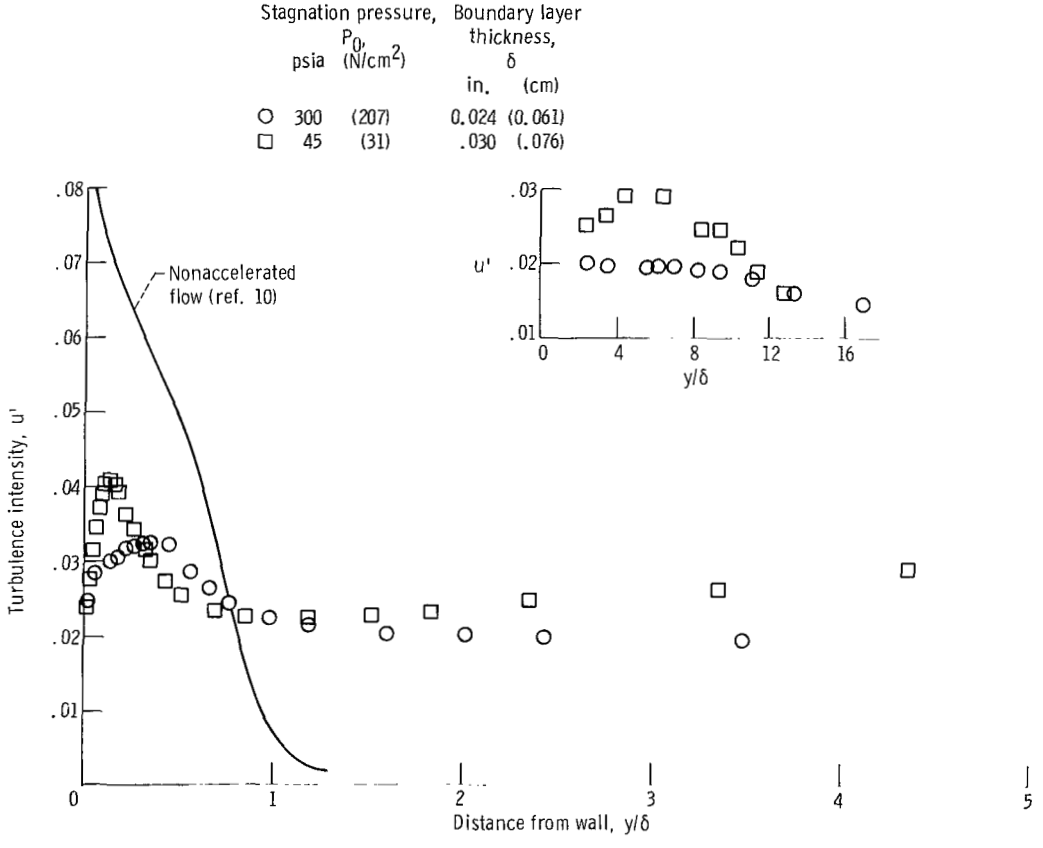

Figure 13. - Experimental distributions of turbulence intensity in nozzle. Mach 0.08; stagnation temperature, 550° R (305 K).

critical level was much higher than the peak value for a normal flat-plate turbulent boundary layer. This high value of peak turbulence intensity was attributed to large rotational fluctuations similar to those occurring in the final stages of natural transition. Similar reasoning might explain the results of this study; however, experimental confirmation cannot be established on the basis of the present information.

The intensity measured by Klebanoff (ref. 10) for a constant pressure flow is also presented in figure 13. The peak intensities measured at both pressure levels are substantially lower than those presented in reference 10. As will be shown, this is a result of the effects of intermittency and the low-level turbulence intensity in the "detrained" layer. As discussed previously, the measured intensity u' is a time-mean quantity and depends not only on the intensity associated with the boundary layer but also on the intensities associated with the "detrained" layer and free stream. In order to compare the intensities of the unaccelerated and accelerated boundary layers it is necessary to determine the value of turbulence intensity associated with the boundary layer u'_{BL}. The value of u'_{BL} can be obtained upon analyzing the components which comprise the turbulent component of the velocity signal $u(t)$. The statistical properties of the signal $u(u \equiv \tilde{u} - U)$ are such that the mean value $\bar{u}$ must be equal to zero. The expressions for u and u^2 are developed in appendix B, and upon making a number of assumptions, the turbulence intensity u' (eq. (B4)) is

$$u' = \left[(1 - \gamma)u'^2_{FS} + (\gamma - \gamma_{BL})u'^2_{DET} + \gamma_{BL}u'^2_{BL}\right]^{1/2}$$

This relation has been used to obtain an estimate of u'_{BL} for only the high-pressure operating condition. The intensity u'_{BL} is compared in figure 14 to the equivalent intensity, $u'_{BL} = u'/\sqrt{\gamma}$, for the constant pressure flow of reference 10. In making the estimate, only the quantities γ and u' were measured directly. The value of free-stream turbulence intensity u'_{FS} is expected to be 0.02 (fig. 13) or less. The value of u'_{DET} extrapolated to $y = 0$ was nearly independent of u'_{FS}, and ranged from 0.023 for $u'_{FS} = 0.02$ to 0.021 for $u'_{FS} = 0.0$. The value of u'_{FS} used in the calculation of u'_{BL} was 0.02. It was assumed that the free-stream turbulence intensity persisted to the wall. The turbulence intensity of "detrained" fluid u'_{DET} was determined by applying the preceding equation to the "detrained" layer to obtain u'_{DET} and then extrapolating the results to the near-wall region. In the "detrained" region $\gamma_{BL} = 0$. The value of γ_{BL} was also deduced from extrapolation of γ in the "detrained" layer to the wall. Very close to the wall these extrapolations must fail because both the "detrained" intermittency and intensity must approach zero. The comparison of intensities of figure 14 is therefore invalid at small values of y/δ. The uncertainty in γ during "laminarization" of the boundary layer prevents a similar estimate at the low-pressure operating

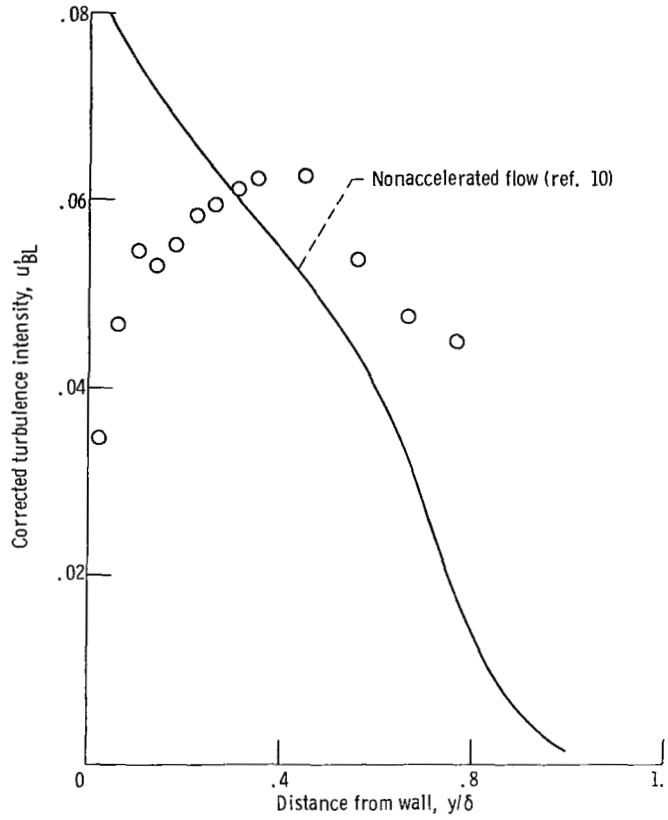

Figure 14. - Distribution of turbulence intensity in nozzle upon accounting for effects of intermittency. Mach 0.08; stagnation temperature, 550° R (305 K); stagnation pressure, 300 psia (207 N/cm^2); boundary layer thickness, 0.024 inch (0.061 cm).

condition. For $y/\delta > 0.4$, the comparison in figure 14 shows that the calculated intensity of the turbulence in the boundary layer is still of the same order as the intensity of the turbulence in a constant pressure boundary layer. Therefore, within the limits of this investigation, the time-average characteristics of the boundary layer, where turbulent and viscous shear effects remain important, are not largely affected by the favorable acceleration. The major effect of large acceleration is to cause "detrainment" of fluid from the boundary layer.

SUMMARY OF RESULTS

A program to study certain characteristics of the turbulence in the boundary layer of a highly accelerated flow has led to the following results:

1. Under conditions of the acceleration often encountered in high-Reynolds-number nozzle flows, the measured profiles of mean velocity, intermittency, and turbulence

intensity are different than classical flat-plate profiles. These differences are the result of a fluid discharge ("detrainment") from the much thicker boundary layer occurring upstream. This causes the boundary layer to develop within the "wake" of its upstream layer.

2. Hot-wire measurements of the time-mean velocity profiles indicated that at a low value of acceleration parameter K (high Reynolds number) the velocity in the inner portion of the profile varies approximately as a 1/7 power. At a high value of K (low Reynolds number), the inner portion of the velocity profile exhibited time-mean characteristics somewhat similar to a laminar profile near the wall followed by a turbulent profile. The outermost portions of the profiles at both the high and low Reynolds numbers reflected the "detrainment" of mass from the upstream boundary layer.

3. Direct measurements of turbulence intensity in the nozzle boundary layer indicated that the peak intensity was only about one-half the values for a flat-plate flow. However, upon correcting for the intermittency, wherein the "detrained" layer was not treated as part of the boundary layer, the measured turbulence intensity profile at a high-Reynolds-number condition was quantitatively similar to the flat-plate profile.

4. The peak value of measured turbulence intensity for the "laminarized" boundary layer was also much lower than the value for a turbulent boundary layer in nonaccelerated flow but higher than the measured peak value for the accelerated turbulent boundary layer. However, since an intermittency correction could not be confidently applied to the turbulence intensity profile at low Reynolds number, the effects of changes in Reynolds number on the turbulence intensity could not be established.

5. The intermittency associated with the accelerated flow was appreciably different than the conventional Gaussian integral curves. For high Reynolds number, the presence of "detrained" fluid caused the intermittency factor to vary as a Gaussian integral curve in the region of turbulent shear near the wall and as a log-normal integral curve in the region containing "detrained" fluid. At low Reynolds number, the intermittency factor varied in a similar manner in the region where "detrainment" occurred. In the region near the wall, "laminarization" caused the intermittency factor to decrease as the wall was approached.

Lewis Research Center,
National Aeronautics and Space Administration,
Cleveland, Ohio, June 9, 1970,
129-01.

APPENDIX A

ANALYTICAL DESCRIPTION OF INTERMITTENCY DISTRIBUTION

For conventional boundary layers the intermittency (fig. 15) is proportional to a complimentary error function. The radial gradient of the intermittency is proportional to the probability density of the instantaneous position of the front between turbulent and nonturbulent fluid. Since the intermittency distribution has been found to be closely approximated by the complimentary error function, the probability density (fig. 15) is Gaussian.

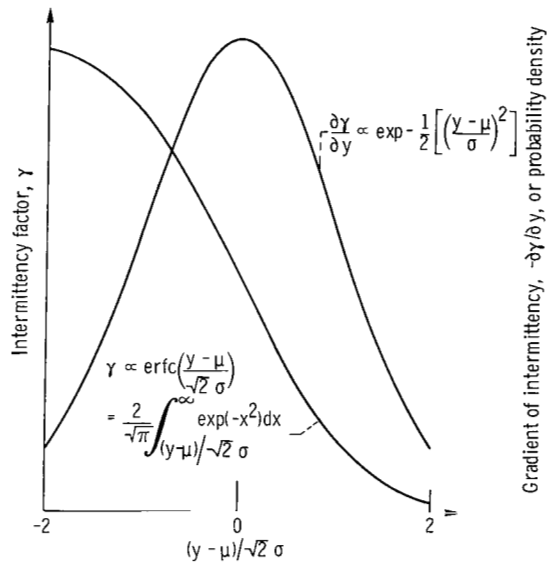

Figure 15. - Intermittency and probability density distribution of conventional boundary layers.

The radial distribution of intermittency for the high-pressure operating condition in the nozzle is given in figure 11. This distribution obviously cannot be approximated by a single complimentary error function as evidenced by the nonlinearity on probability paper. The measured distribution of intermittency was characterized by an abrupt change in slope near the wall and the presence of a double maximum in the probability density distribution (fig. 16). The data are therefore fitted to two separate distributions, one for a radial distance less than 0.024 inch (0.061 cm) and the other for the outer region.

In the outer region, the nonlinearity of the intermittency distribution implies that the probability density distribution is not symmetric about some mean value of radial

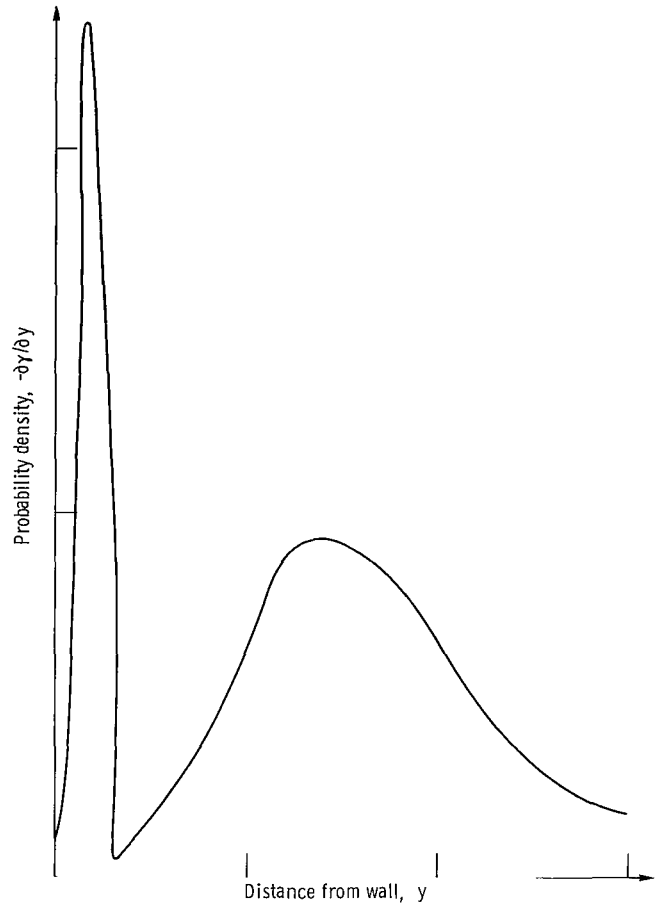

Figure 16. - Radial distribution of probability density in nozzle.

distance. The radial variation of $-\partial\gamma/\partial y$ becomes nearly symmetric, however, when considered to be a function of the log of y. It can therefore be fitted quite well by a log-normal distribution.

A log-normal distribution can be expressed as a normal distribution of the log of y where the log function is

$$g(\ln y) = K_1 \exp\left(\frac{\ln y - \mu}{K_2}\right)^2$$

The mean μ is given by the mean of ln y, and the constants K_1 and K_2 are expressed in terms of the standard deviation σ and a normalization constant A. The area under the entire curve of the probability density distribution must be unity. Since the log-normal distribution characterizes only the outer part of the distribution, it must be

normalized to a value A which represents the fraction of the total area associated with the log-normal distribution. Evaluation of the constants K_1 and K_2 then gives

$$g(\ln y) = \frac{A^{3/2}}{\sqrt{2\pi}\,\sigma} \exp\left(-\frac{A}{2}\right)\left(\frac{\ln y - \overline{\ln y}}{\sigma}\right)^2$$

The standard deviation can be expressed in terms of characteristics of the measured distribution of intermittency by

$$\sigma = \frac{A^{3/2}}{\sqrt{2\pi}\, e^{\overline{\ln y}}} \left(-\left.\frac{\partial\gamma}{\partial y}\right|_{y=e^{\overline{\ln y}}}\right)^{-1}$$

The log-normal distribution can then be expressed as

$$-\frac{\partial\gamma}{\partial y} \equiv f(y) = \frac{e^{\overline{\ln y}}}{y}\left(-\left.\frac{\partial\gamma}{\partial y}\right|_{y=e^{\overline{\ln y}}}\right) \exp -\left\{\pi\left[-\left.\frac{\partial\gamma}{\partial y}\right|_{y=e^{\overline{\ln y}}} \frac{e^{\overline{\ln y}}}{A}(\ln y - \overline{\ln y})\right]^2\right\} \quad \text{(A1)}$$

Integration then gives the intermittency distribution for $y > 0.024$ inch (0.061 cm)

$$\gamma_{DET} = \frac{A}{2}\,\mathrm{erfc}\left[\sqrt{\pi}\,\frac{e^{\overline{\ln y}}}{A}\left(-\left.\frac{\partial\gamma_{DET}}{\partial y}\right|_{y=e^{\overline{\ln y}}}\right)(\ln y - \overline{\ln y})\right] \quad \text{(A2)}$$

The value of A can be obtained either from the definition or from the γ-distribution by extrapolation to $y = 0$ since

$$A = \gamma_{DET,\, y=0} \quad \text{(A3)}$$

Equation (A3) is generally preferred because it is less susceptible to experimental error. For the intermittency distribution of figure 12, the extrapolation of the γ-distribution to the wall gives a value of $\gamma_{DET,\, y=0} = 0.81$.

From the definition, the value of A was also obtained by first differentiating the experimental distribution of intermittency. These results, cast in the form of the probability density, were then integrated to give a value of 0.76 for A.

The region of the intermittency distribution for $y < 0.024$ inch (0.061 cm) closely fits a conventional error function representation. The probability density distribution

associated with the intermittency must however be normalized to (1.0 - A) instead of unity. This results in

$$\gamma\left(0 < \frac{y}{\delta} < 1.0\right) \equiv \gamma_{BL} = \frac{2\gamma_{BL,\, y=\bar{y}_{BL}}}{\sqrt{\pi}} \int_{\chi}^{\infty} \exp - \chi^2 \, dx$$

where

$$\chi = \sqrt{\frac{1 - A}{2}} \frac{y - \bar{y}_{BL}}{\sigma}$$

Finally,

$$\gamma_{BL} = \gamma_{BL,\, y=\bar{y}_{BL}} \operatorname{erfc} \sqrt{\frac{1 - A}{2}} \frac{y - \bar{y}_{BL}}{\sigma} \tag{A4}$$

The boundary layer has a mean of 0.8 δ and a standard deviation of 0.12 δ. These values are dependent on the value of A selected.

The standard deviation σ can also be expressed in terms of characteristics of the intermittency distribution to give

$$\gamma_{BL} = \frac{1 - \gamma_{DET,\, y=0}}{2} \operatorname{erfc}\left(\sqrt{\pi} \frac{\bar{y}_{BL} - y}{1 - \gamma_{DET,\, y=0}} \left. \frac{\partial \gamma_{BL}}{\partial y} \right|_{y=\bar{y}_{BL}} \right) \tag{A5}$$

Since the probability density distribution is normalized, the two intermittency distributions are additive and the complete distribution is given by

$$\gamma = \frac{\gamma_{DET,\, y=0}}{2} \operatorname{erfc}\left[\frac{\sqrt{\pi}\, e^{\overline{\ln y}}}{\gamma_{DET,\, y=0}} \left(- \left. \frac{\partial \gamma_{DET}}{\partial y} \right|_{y=e^{\overline{\ln y}}} \right) (\ln y - \overline{\ln y}) \right]$$

$$+ \frac{1 - \gamma_{DET,\, y=0}}{2} \operatorname{erfc}\left(\sqrt{\pi} \frac{\bar{y}_{BL} - y}{1 - \gamma_{DET,\, y=0}} \left. \frac{\partial \gamma_{BL}}{\partial y} \right|_{y=\bar{y}_{BL}} \right) \tag{A6}$$

The first term of equation (A6) represents the contribution from the log-normal distribution and is negligible within the boundary layer (where the viscous effects are important). Likewise, the second term has a negligible contribution outside the boundary layer and represents the contribution from the normal distribution.

APPENDIX B

RELATION BETWEEN TURBULENCE PROPERTIES AND INTERMITTENT SIGNAL

In a nonaccelerated boundary layer, there exists at any point in the wake region a mixed flow composed of flow with free-stream turbulence and a flow with wall shear turbulence. Each type of flow is separated by a sharp instantaneous demarcation. In general, the turbulence associated with the free-stream type of turbulent flow is much weaker than that associated with the wall shear type of turbulence.

When a fixed probe is placed in such a mixed flow, the probe will react alternately to each type of turbulent flow as it is swept by. Any time average measurement, such as intensity, can therefore be interpreted as an average of two averaged values. That is, the averaged measurement during the free-stream type turbulence is averaged with the average measurement during the wall shear type turbulence. In a study of wall shear turbulence it is necessary to account for the effect of free-stream turbulence when interpreting experimental measurements in the wake regions of boundary layers.

In a strongly accelerated boundary layer the mixed flow in the wake region is further complicated by the presence of the "detraining" fluid. When "detrainment" exists, the mixed flow region is then composed of three types of flow. In addition to the flows with free-stream type turbulence and wall shear type turbulence, a flow with turbulence characteristic of the "detrained" layer is present. A fixed probe then averages the conditions associated with each of the three flow regimes.

In a study of the acceleration effect on the turbulent intensity of wall shear flow, the time averaged intensity measurements of the mixed flow must be corrected for the effects of the component flows with free-stream and "detrainment" type turbulence. Similar corrections have previously been considered by Townsend (ref. 13) and Corrsin (ref. 8). In this appendix, a relation will be developed for the turbulent intensity of the part of the mixed flow due to wall shear. This turbulent intensity will be expressed in terms of (1) the measured turbulent intensity of the entire mixed flow, (2) the measured intermittency of the mixed flow, (3) the turbulent intensity of the part of the mixed flow resulting from "detrained" flow, (4) the turbulent intensity of the part of the mixed flow resulting from free-stream type flow, and (5) the fraction of time that wall shear flow is present in the mixed flow. The analysis is an extension of that given by Corrsin in reference 8.

In the mixed flow under consideration, there is a sharp demarcation between each of the three component flows. The total instantaneous velocity signal $\tilde{u}(t)$ in figure 17(d), can therefore be expressed as a sum of three instantaneous signals of the type indicated in figures 17(a) to (c). Each of these three instantaneous signals has a finite nonzero

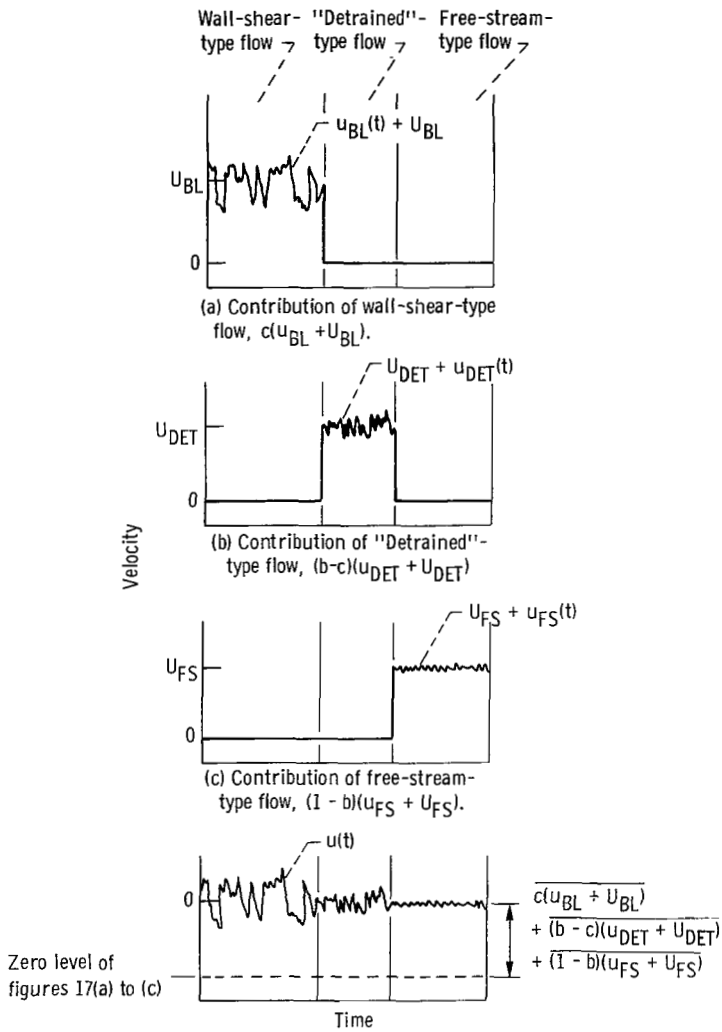

Figure 17. - Velocity components comprising total velocity signal u(t).

contribution only during that time when the flow which it represents is present in the mixed flow.

Before proceeding with the analytical representation of the total instantaneous velocity signal $\tilde{u}(t)$, it is necessary to define the signals and parameters which $\tilde{u}(t)$ depends upon. In figure 17(a), there is a nonzero time-dependent contribution only during the time when wall shear flow is present in the mixed flow. We define an arbitrary zero reference such that the mean of the nonzero time-dependent contribution of the signal in figure 17(a) is U_{BL}. This also defines the zero level for the velocity signals depicted in figures 17(b) and (c). In figure 17(b), the mean of the nonzero time-dependent part of the signal associated with "detraining" flow is U_{DET}. Likewise, in figure 17(c), the

mean of the nonzero time-dependent part of the signal associated with free-stream type flow is U_{FS}.

In figure 17(a), a hypothetical velocity signal $u_{BL}(t)$ is defined such that it has the same physical characteristics as the measured nonzero time-dependent velocity distribution of the shear flow part of the mixed flow. It is assumed that this hypothetical velocity $u_{BL}(t)$ has a zero mean value. The difference between the mean of $u_{BL}(t)$ and the previous defined zero reference is therefore U_{BL}. In a study of the acceleration effect on the turbulent intensity of wall shear, the intensity associated with $u_{BL}(t)$ should be compared with the corresponding intensity associated with $u_{BL}(t)$ of the nonaccelerated flow. It is the objective of this analysis therefore to find a relation between $\overline{u_{BL}^2(t)}$ and the various other mean-square velocity signals which comprise $\overline{u^2(t)}$.

It is also necessary to introduce an on-off signal before the signal in figure 17(a) can be analytically represented. A signal c(t) is therefore defined such that it has the value 1.0 whenever the signal in figure 17(a) has a nonzero contribution and has the value 0.0 at all other times. Although this on-off signal has no physical significance, its mean represents the fraction of time that wall shear type flow is present in the mixed flow. This fraction is the intermittency factor γ_{BL} of the boundary layer.

The signal in figure 17(a) can now be analytically represented in terms of the hypothetical velocity signal and the on-off signal as $c(t)[u_{BL}(t) + U_{BL}]$. The analytical representation of the contribution of the "detrained" flow and the free-stream flow parts of the mixed flow to the total velocity signal $\tilde{u}(t)$ follows a similar development.

Referring to figures 17(b) and (c), it is again necessary to define hypothetical velocities for both the "detrained" and free-stream type flows. It is assumed that each of these hypothetical velocities has the same physical characteristics as the measured nonzero time-dependent velocity distributions of the "detrained" part of the free-stream type parts of the mixed flow. The signal which represents the "detrained" fluid is $u_{DET}(t)$, and that which represents the free-stream type fluid is $u_{FS}(t)$. Again it is assumed that the mean of each signal, i.e. $\overline{u_{DET}(t)}$ and $\overline{u_{FS}(t)}$, is zero. As indicated in figures 17(b) and (c), the difference between the mean of the hypothetical velocity signal and the zero reference is given by the parameters U_{DET} and U_{FS}.

It is also necessary to define an additional on-off signal. This on-off signal b(t) is defined as 1.0 when either wall shear type flow or "detrained" flow is present and is 0.0 at all other times. Again the on-off signal has no physical significance, but the mean represents the fraction of time that either "detrained" fluid or wall shear type fluid is present in the mixed flow. This mean is the measured intermittency factor γ. Obviously γ is always larger than γ_{BL}.

It is now possible to analytically represent the velocity signals of figures 17(b) and (c). The signal in figure 17(b) can be represented by $[b(t) - c(t)][u_{DET}(t) + U_{DET}]$, and the signal in figure 17(c) can be represented as $[1 - b(t)][u_{FS}(t) - U_{FS}]$. The sum of the

signals given in figures 17(a) to (c) represents a velocity signal which is similar to the desired total instantaneous velocity signal $\tilde{u}(t)$ The fluctuating component of the instantaneous velocity $u(t)$ must have a zero mean, whereas the sum of the signals in figures 17(a) to (c) do not. To form $u(t)$, therefore, subtract the mean of the sum from the sum of the signals of figures 17(a) to (c). The combined fluctuating component of the instantaneous velocity signal $u(t)$ is then given by

$$u(t) = c(t)[u_{BL}(t) - U_{BL}] + [b(t) - c(t)][u_{DET}(t) + U_{DET}]$$

$$+ [1 - b(t)][u_{FS}(t) - U_{FS}] - \overline{c(t)[u_{BL}(t) - U_{BL}]}$$

$$- \overline{[b(t) - c(t)][u_{DET}(t) + U_{DET}]} - \overline{[1 - b(t)][u_{FS}(t) - U_{FS}]}$$

If each time-dependent velocity can be assumed to be statistically independent of the other velocities and the on-off signals, the mean square value of $u(t)$ can be written as

$$\overline{u^2} = \bar{c}\overline{u_{BL}^2} + (1 - \bar{b})\overline{u_{FS}^2} + (\bar{b} - \bar{c})\overline{u_{DET}^2} - \bar{b}(1 - \bar{b})U_{FS}^2 + [\bar{b} - \bar{c} - (\bar{b} - \bar{c})^2]U_{DET}^2$$

$$+ (\bar{c} - \bar{c}^2)U_{BL}^2 - 2(1 - \bar{b})(\bar{b} - \bar{c})U_{DET}U_{FS}$$

$$- 2\bar{c}(1 - \bar{b})U_{FS}U_{BL} - 2\bar{c}(\bar{b} - \bar{c})U_{BL}U_{DET} \quad \text{(B1)}$$

Now when the mean velocities during each of the three flow modes are equal, equation (B1) reduces to a simple form somewhat similar to the form suggested by Townsend. No information is available concerning the time-mean velocities in equation (B1). However, they should not, in general, be equal. Nevertheless, for simplicity it is felt that a semi-quantitative estimate can be made by assuming the three time-average velocities to be equal. Equation (B1) then becomes

$$\overline{u^2} = \bar{c}\overline{u_{BL}^2} + (1 - \bar{b})\overline{u_{FS}^2} + (\bar{b} - \bar{c})\overline{u_{DET}^2} \quad \text{(B2)}$$

This can now be expressed in terms of (1) the intermittency factor γ_{BL}, which is the fraction of time that boundary layer turbulence is present and (2) the intermittency factor γ, which is the fraction of time that either boundary layer or "detrained" layer is present.

$$\overline{u^2} = \gamma_{BL}\overline{u^2_{BL}} + (1 - \gamma)\overline{u^2_{FS}} + (\gamma - \gamma_{BL})\overline{u^2_{DET}} \tag{B3}$$

Equation (B3) can be expressed in terms of the turbulence intensity u' as follows:

$$u' = \left[\gamma_{BL}u'^2_{BL} + (1 - \gamma)u'^2_{FS} + (\gamma - \gamma_{BL})u'^2_{DET}\right]^{1/2} \tag{B4}$$

APPENDIX C

SYMBOLS

A	constant of normalization (appendix A)
b	random on-off signal taken as either 0 or 1.0
C	constant
C_f	skin friction coefficient
c	random on-off signal taken as either 0 or 1.0
K	acceleration parameter, $K = (\nu_\infty/U_\infty^2)(dU_\infty/dx)$
K_{crit}	critical value of acceleration parameter, $K_{crit} \approx 3\times10^{-6}$
K_1 and K_2	constants (appendix A)
$\dot{m}$	mass flow in boundary layer
Pr	Prandtl number
P_0	stagnation pressure
$Re_{d,r}$	Reynolds number based on diameter (properties evaluated at reference temperature)
St_r	Stanton number (properties evaluated at reference temperature)
T_0	stagnation temperature
U	time-mean value of local velocity
U_{BL}	time-mean value of velocity for the wall shear type flow of a mixed flow
U_{DET}	time-mean value of velocity for "detrained" fluid of a mixed flow
U_{FS}	time-mean value of velocity for free-stream fluid of a mixed flow
U_∞	time-mean value of free-stream velocity
u	fluctuating component of instantaneous velocity parallel to wall
$\tilde{u}$	instantaneous velocity parallel to wall
u^+	dimensionless velocity, $u^+ = (U/U_\infty)/\sqrt{(C_f/2)(\rho_\infty/\rho_w)}$
u'	measured turbulence intensity, $u' = \sqrt{\overline{u^2}}/U_\infty$
u_{BL}	hypothetical instantaneous velocity identical with velocity of wall shear type portion of mixed flow
u_{DET}	hypothetical instantaneous velocity identical with velocity of "detrained" type portion of mixed flow
u_{FS}	hypothetical instantaneous velocity identical with velocity of free-stream type portion of mixed flow
v	instantaneous velocity normal to wall

x	distance along wall
y	distance from wall
y^+	dimensionless distance from wall, $y^+ = (U_\infty y/\nu_w)\sqrt{(C_f/2)(\rho_\infty/\rho_w)}$
$\overline{y}_{BL}$	mean position of turbulence front in boundary layer
γ	measured intermittency factor; percent of time boundary layer and/or "detrained" layer is present
γ_{BL}	intermittency factor; percent of time boundary layer is present
γ_{DET}	intermittency factor; percent of time "detrained" layer is present
$\gamma_{DET,y=0}$	intermittency factor for "detrained" layer extrapolated to $y = 0$
δ	boundary layer thickness
δ^*	displacement thickness
θ	momentum thickness
μ	mean value of y or $\ln y$
ν_w	wall value of kinematic viscosity
ν_∞	free-stream value of kinematic viscosity
ρ	density
$\rho\overline{uv}$	turbulent shear stress
ρ_∞	free-stream value of density
ρ_w	wall value of density
σ	standard deviation of $y - \overline{y}$ or $\ln y - \overline{\ln y}$
τ	time
χ	nondimensional grouping, $\chi \equiv \sqrt{(1 - A)/2}\,(y - \overline{y}_{BL})/\sigma$

Superscript:

$\overline{\ }$	mean value

REFERENCES

1. Moretti, P. M.; and Kays, W. M.: Heat Transfer Through an Incompressible Turbulent Boundary Layer with Varying Free-Stream Velocity and Varying Surface Temperature. Rep. PG-1, Thermosciences Div., Mech. Eng. Dept., Stanford Univ., Nov. 1964.

2. Launder, B. E.: Laminarization of the Turbulent Boundary Layer in a Severe Acceleration. J. Appl. Mech., vol. 31, no. 4, Dec. 1964, pp. 707-708.

3. Launder, B. E.; and Stinchcombe, H. S.: Non-Normal Similar Turbulent Boundary Layers. Rep. TWF/TN/21, Imperial College of Science and Technology, London, May 1967.

4. Boldman, Donald R.; Schmidt, James F.; and Gallagher, Anne K.: Laminarization of a Turbulent Boundary Layer as Observed from Heat-Transfer and Boundary-Layer Measurements in Conical Nozzles. NASA TN D-4788, 1968.

5. Back, L. H.; Cuffel, R. F.; and Massier, P. F.: Laminarization of a Turbulent Boundary Layer in Nozzle Flow-Boundary Layer and Heat Transfer Measurements with Wall Cooling. Paper 69-HT-56, ASME, Aug. 1969.

6. Brinich, P. F.; and Neumann, H. E.: Some Effects of Acceleration on the Turbulent Boundary Layer. AIAA J., vol. 8, no. 5, May 1970, pp. 987-989.

7. Bradbury, L. J. S.: A Simple Circuit for the Measurement of the Intermittency Factor in a Turbulent Flow. Aeronautical Quart., vol. 15, no. 3, Aug. 1964, pp. 281-284.

8. Corrsin, Stanley; and Kistler, Alan L.: The Free-Stream Boundaries of Turbulent Flows. NACA TN 3133, 1953.

9. Bradshaw, P.: Negative Entrainment in Turbulent Shear Flow. Rep. NPL-Aero-1249, National Physical Lab., England, Oct. 16, 1967.

10. Klebanoff, P. S.: Characteristics of Turbulence in a Boundary Layer with Zero Pressure Gradient. NACA TR 1247, 1955.

11. Bradshaw, P.; and Ferriss, D. H.: The Response of a Retarded Equilibrium Turbulent Boundary Layer to the Sudden Removal of Pressure Gradient. NPL-Aero-1145, National Physical Lab., England, Mar. 16, 1965.

12. Baronti, P. O.: An Investigation of the Turbulent Incompressible Boundary Layer. Tech. Rep. 624, General Applied Science Lab., May 1967.

13. Townsend, A. A.: The Structure of Turbulent Shear Flow. Cambridge University Press, 1956.

NASA-Langley, 1970 —— 12 E-5689

NATIONAL AERONAUTICS AND SPACE ADMINISTRATION
WASHINGTON, D. C. 20546
OFFICIAL BUSINESS

FIRST CLASS MAIL

POSTAGE AND FEES PAID
NATIONAL AERONAUTICS AN
SPACE ADMINISTRATION

04U 001 37 51 3DS 70272 00903
AIR FORCE WEAPONS LABORATORY /WLOL/
KIRTLAND AFB, NEW MEXICO 87117

ATT E. LOU BOWMAN, CHIEF, TECH. LIBRARY

POSTMASTER: If Undeliverable (Section 158 Postal Manual) Do Not Retur

"The aeronautical and space activities of the United States shall be conducted so as to contribute . . . to the expansion of human knowledge of phenomena in the atmosphere and space. The Administration shall provide for the widest practicable and appropriate dissemination of information concerning its activities and the results thereof."

— NATIONAL AERONAUTICS AND SPACE ACT OF 1958

NASA SCIENTIFIC AND TECHNICAL PUBLICATIONS

TECHNICAL REPORTS: Scientific and technical information considered important, complete, and a lasting contribution to existing knowledge.

TECHNICAL NOTES: Information less broad in scope but nevertheless of importance as a contribution to existing knowledge.

TECHNICAL MEMORANDUMS: Information receiving limited distribution because of preliminary data, security classification, or other reasons.

CONTRACTOR REPORTS: Scientific and technical information generated under a NASA contract or grant and considered an important contribution to existing knowledge.

TECHNICAL TRANSLATIONS: Information published in a foreign language considered to merit NASA distribution in English.

SPECIAL PUBLICATIONS: Information derived from or of value to NASA activities. Publications include conference proceedings, monographs, data compilations, handbooks, sourcebooks, and special bibliographies.

TECHNOLOGY UTILIZATION PUBLICATIONS: Information on technology used by NASA that may be of particular interest in commercial and other non-aerospace applications. Publications include Tech Briefs, Technology Utilization Reports and Notes, and Technology Surveys.

Details on the availability of these publications may be obtained from:

SCIENTIFIC AND TECHNICAL INFORMATION DIVISION

NATIONAL AERONAUTICS AND SPACE ADMINISTRATION

Washington, D.C. 20546